TISSUE ENGINEERING: Part A
Volume 26, Numbers 13 and 14, 2020

DOI: 10.1089/ten.tea.2020.0040

termis
Tissue Engineering
& Regenerative Medicine
International Society

SPECIAL ISSUE ON WOMEN'S HEALTH

Sex-Dependent Macromolecule and Nanoparticle Delivery in Experimental Brain Injury

Vimala N. Bharadwaj, PhD,[1] Connor Copeland, BS,[1] Ethan Mathew, MS,[1]
Jason Newbern, PhD,[2] Trent R. Anderson, PhD,[3] Jonathan Lifshitz, PhD,[4–6]
Vikram D. Kodibagkar, PhD,[1] and Sarah E. Stabenfeldt, PhD[1]

The development of effective therapeutics for brain disorders is challenging, in particular, the blood-brain barrier (BBB) severely limits access of the therapeutics into the brain parenchyma. Traumatic brain injury (TBI) may lead to transient BBB permeability that affords a unique opportunity for therapeutic delivery via intravenous administration ranging from macromolecules to nanoparticles (NPs) for developing precision therapeutics. In this regard, we address critical gaps in understanding the range/size of therapeutics, delivery window(s), and moreover, the potential impact of biological factors for optimal delivery parameters. Here we show, for the first time, to the best of our knowledge, that 24-h postfocal TBI female mice exhibit a heightened macromolecular tracer and NP accumulation compared with male mice, indicating sex-dependent differences in BBB permeability. Furthermore, we report for the first time the potential to deliver NP-based therapeutics within 3 days after focal injury in both female and male mice. The delineation of injury-induced BBB permeability with respect to sex and temporal profile is essential to more accurately tailor time-dependent precision and personalized nanotherapeutics.

Keywords: sex-dependence, blood-brain barrier, nanoparticle, traumatic brain injury, drug delivery, intravital microscopy

Impact Statement

In this study, we identified a sex-dependent temporal profile of blood/brain barrier disruption in a preclinical mouse model of traumatic brain injury (TBI) that contributes to starkly different macromolecule and nanoparticle delivery profiles post-TBI. The implications and potential impact of this work are profound and far reaching as it indicates that a demand of true personalized medicine for TBI is necessary to deliver the right therapeutic at the right time for the right patient.

Introduction

The development of effective therapeutics for brain disorders, such as traumatic brain injury (TBI), remains a major clinical challenge.[1,2] In particular, the blood-brain barrier (BBB) severely limits access of the therapeutics into the brain parenchyma.[1] Due to its highly selective nature, the BBB constitutes the greatest impediment for drug delivery via blood circulation to treat brain disorders. As such, several active drug delivery strategies such as transient BBB disruption via focused ultrasound and convection-enhanced delivery are being explored in preclinical settings to facilitate drugs/macromolecules to cross or bypass the BBB.[3] These tools are useful, yet, certain neural pathologies may naturally afford the ability to exploit periods of enhanced BBB permeability for enabling drug delivery to the parenchyma.

For example, TBI may lead to a transient BBB disruption that affords a unique opportunity for the development of precision therapeutics via intravenous administration, thus facilitating a spectrum of therapeutics ranging from macromolecules to nanoparticles (NPs). However, there is a critical gap in understanding the permissible range/size of

[1]School of Biological and Health Systems Engineering, Ira A. Fulton Schools of Engineering, Arizona State University, Tempe, Arizona, USA.
[2]School of Life Sciences, Arizona State University, Tempe, Arizona, USA.
[3]Basic Medical Sciences, University of Arizona, College of Medicine–Phoenix, Phoenix, Arizona, USA.
[4]Department of Child Health, University of Arizona, College of Medicine–Phoenix, Phoenix, Arizona, USA.
[5]BARROW Neurological Institute at Phoenix Children's Hospital, Phoenix, Arizona, USA.
[6]Phoenix VA Health Care System, Phoenix, Arizona, USA.

therapeutic agents, optimal delivery window(s), and moreover, the potential impact of biological factors on BBB permeability after a TBI and ultimately therapeutic delivery parameters. Therefore, in this study, we characterize three crucial factors (1) size range (macromolecules vs. NPs) for therapeutics, (2) their temporal profiles (acute and subacute postinjury delivery), and (3) sex dependence (female vs. male) that can directly influence the accumulation within injured brain tissue.

Brain injury is characterized by structural failure and neurologic dysfunction that begins at the time of impact and lasting for hours to weeks.[4,5] The primary injury is the direct result of the initial trauma of a TBI and leads to an indirect secondary injury, a cascade of neural and vascular events, including inflammation, edema, and BBB disruption.[4,5] The secondary injury develops over hours and days following a TBI allowing a time window for intervention. Most consequences of BBB disruption after brain injury are known to be detrimental, yet the disruption may also provide a transient window for delivery of therapeutics that normally would not cross this barrier from the systemic circulation.[6–9]

Macromolecules such as specific antibodies and proteins have been identified as promising therapeutic agents for the treatment of various brain pathologies.[1,10] These therapeutic agents can exert numerous biological actions in the brain such as regulation of cerebral blood flow, neurotransmission, and neuromodulation.[10] Furthermore, in recent years, NPs have been used extensively to serve as carriers for improved drug stability, pharmacokinetics, and therapeutic efficacy with reduced toxicity.[9,11,12]

The abovementioned classes of therapeutics, including proteins[13,14] and NPs,[15,16] have been approved by the U.S. Food and Drug Administration for clinical use for other diseases/pathologies. However, there is a critical gap in understanding the utility of using both classes of therapeutics for brain injury since the delivery parameters for optimal and personalized delivery (i.e., the impact of biological factors) have not been previously investigated. Therefore, in this preclinical study, we use large-molecular-weight (MW) protein tracers ($\sim$40 kDa, horseradish peroxidase [HRP]) and NPs ($\sim$40 nm, poly (ethylene glycol) [PEG]ylated fluorescent polystyrene NP) to address this critical gap and as a proof of concept to characterize the delivery profile to the injured brain tissue via the disrupted BBB.

Previously, we and others have established in both focal and diffuse injury models of TBI that macromolecular weight tracer ($\sim$40 kDa)[17–21] and NPs[8,19,20,22–25] robustly accumulate within injured brain tissue in the first 4 h following TBI. Moreover, seminal TBI studies in male rodents suggest a biphasic BBB opening to macromolecular weight tracers with the first peak at acute ($\sim$3–6 h) time points followed by a delayed opening ($\sim$3 days) after TBI.[6,17] However, the potential to deliver larger therapeutics such as NPs beyond 24 h postinjury has not been investigated. Furthermore, sex differences are known to play a role in the morbidity and mortality after TBI,[26,27] yet the underlying mechanisms are not well elucidated.

Sex-specific preclinical studies have reported less BBB disruption in female rodents compared with males within 6 h of injury,[27,28] but no difference 24 h and 7 days postinjury.[29,30] However, sex differences in BBB disruption during clinically important subacute time points between 24 h and 7 days after TBI have not been studied. Taken together, this study aims to characterize a therapeutic window for delivery of large MW tracer and NPs beyond 24 h postinjury. Moreover, we aim to evaluate potential sex-dependent differences in BBB disruption and the subsequent large MW tracer and NP accumulation following TBI. Ultimately, we reveal not only an extended NP delivery window but also key sex-dependent considerations for both large MW tracer and NP delivery strategies following TBI.

Materials and Methods

Materials

Carboxylated polystyrene NPs of 40 nm (F8793) size with red ($\lambda_{ex}/\lambda_{em}$ = 580 nm/605 nm) were purchased from Life Technologies (Carlsbad, CA). Methoxypolyethylene glycol amine 2000 (mPEG-amine 2 kDa) (06676), n-[3-dimethylaminopropyl]-n-ethyl, n-[3-dimethylaminopropyl]-n-ethyl [EDC] (E1769), MES hemisodium buffer (M8902), N-hydroxysuccinimide (NHS) (56405), and peroxidase type II from horseradish (P8250-50KU) were purchased from Sigma Aldrich (St. Louis, MO). ImmPACT DAB peroxidase (HRP) substrate (SK-4105) was purchased from Vector Laboratories (Burlingame, CA). Slide-A-Lyzer Cassettes (20 K) (66003) were purchased from Thermo Fisher Scientific (Waltham, MA). Vectashield antifade mounting medium (H-1000) was purchased from Vector Laboratories. Anti-GFAP (ab53554) was purchased from Abcam (Cambridge, MA). Alexa Fluor 647 secondary (ab150131) was purchased from Abcam.

Nanoparticle poly (ethylene glycol) conjugation

As presented in our previous study,[19,20] carboxylated NPs were PEGylated using EDC/NHS chemistry. Briefly, mPEG-amine 2 kDa was mixed with 40 nm (NH_2:COOH at 5:1 mole excess). EDC/NHS (in MES buffer) was added to the NP/PEG mixture (200 mM/100 mM) and HEPES buffer was added to obtain a final pH of 7.8 before incubating for 3 h at room temperature. Glycine (100 mM) was added to quench the reaction. Unbound PEG was removed via dialysis (20 kDa MW). PEGylated NPs were suspended in 20 mM HEPES (pH 7.4). The concentration of NP solution was determined with fluorescent standard curves generated from known concentrations of as-received fluorospheres (FLUOstar Omega fluorescence plate reader; BMG Labtech, Ortenberg, Germany). Yields of NPs ranged between 40% and 60%. A concentration of 12.5 mg/mL for each NP was used for all *in vivo* studies.

NP characterization

The size (in nanometers) and surface charge (zeta potential in millivolts) of the pre- and post-PEGylation of NPs were evaluated using a Zeta Sizer Nano-ZS (Malvern Instruments, Malvern, United Kingdom). Each NP sample in 20 mM HEPES (pH 7.4) was measured three times consecutively. Three measurements were made and the mean ± standard deviation was reported. To study the stability of the NP for 3 h postinjection, unPEGylated NPs and PEGylated NPs were diluted in serum (incubated at 37°C and 5% CO_2 for at least 2 h before use) at a concentration comparable to the *in vivo* blood concentration (0.42 mg/mL). The samples

were then incubated in a 96-well plate at 37°C and 5% CO_2 incubator for about 3 h and the aggregation was monitored by measurement of absorbance at 320 nm at 37°C.

Nuclear magnetic resonance characterization

The conjugation of PEG and the total quantity on NPs were detected by ^{1}H nuclear magnetic resonance (NMR) spectra analysis using a previously published methodology.[31] PEGylated and unPEGylated polystyrene NPs were weighed and fully dissolved in a mixture of chloroform ($CDCl_3$; Sigma), trifluoroacetic acid-d (TFAd; Sigma), and a known concentration of bis(trimethylsilyl) benzene (BTSB, Sigma) (0.5% w/v). ^{1}H NMR spectra were obtained at 400 MHz using a Varian, Inc. (Palo Alto, CA) VNMRS 500 MHz NMR spectrometer with a 5 mm ID-PFG probe. PEG2000 polymer (3.6 ppm) was dissolved in the same $CDCL_3$-TFAd solvent with BTSB (0.5% w/v) and was made at different concentrations to obtain a calibration curve. Total PEG quantity in the PEGylated NP was calculated using the calibration curve.

Animals

Female and male adult C57BL/6 mice (Jackson Laboratory) aged 8–10 weeks (20–24 g) were used for the HRP extravasation, NP accumulation, and immunohistochemistry analysis experiments ($n=4$ per group). Female and male adult transgenic CX3CR1-GFP (Jackson Laboratory) mice bred with C57BL/6 mice (Jackson Laboratory) were used for two-photon microscopy experiments ($n=3$ per group). Another second cohort of female and male adult C57BL/6 mice aged 8–10 weeks (20–24 g) were used for magnetic resonance imaging (MRI) lesion volume analysis and biodistribution and blood plasma concentration analysis ($n=5$).

Mice were housed in a 14-h light/10-h dark cycle at a constant temperature (23°C ± 2°C) with food and water available *ad libitum*. Female mice of random cycling were used. Animal studies using C57BL/6 mice were approved by Arizona State University's Institutional Animal Use and Care Committee (IACUC) and were performed in accordance with the relevant guidelines. The two-photon microscopy study using transgenic animals was approved by the Institutional Animal Care and Use Committee at the University of Arizona (Tucson, AZ).

Controlled cortical impact model

TBI was modeled using the well-established controlled cortical impact (CCI) injury model.[32] Briefly, anesthetized (isoflurane) adult mice were mounted onto a stereotaxic frame. The frontoparietal cortex was exposed via 3–4 mm craniotomy and the impact tip was centered to the craniectomy. The impactor tip diameter was 2 mm, the impact velocity was 6.0 m/s, and the depth of cortical deformation was 2 mm and 100 ms impact duration (Impact ONE; Leica Microsystems). The skin was sutured and the animals were placed in a 37°C incubator until consciousness was regained. The sham group went through the same protocol but did not receive the impact injury.

NP and horseradish peroxidase injection

Retro-orbital injections of the venous sinus in the mouse, an alternative technique to tail-vein injection,[33] were performed for intravenous delivery of the NPs and HRP. Animals were anesthetized with isoflurane (3%) and received intravenous NP injections (30 mg/kg b.w. 50 μL; retro-orbital) of 40 nm NPs 3 h before perfusion. HRP (83 mg/kg b.w.in 25 μL) was retro-orbitally injected behind the second eye 10 min before perfusion. Depending on the cohort group, animals were sacrificed at 3 h, 24 h, 3 days, or 7 days postinjury. The NP circulation time of 3 h was held constant for all cohorts. The summary of the experimental time line is depicted in Supplementary Figure S1.

Tissue collection

At the end time point, mice were deeply anesthetized with a lethal dose of sodium pentobarbital solution. After the loss of a tail/toe pinch reflex movement, animals were transcardially perfused with cold phosphate-buffered saline (PBS), followed by 4% buffered paraformaldehyde solution. Brain tissue was collected and fixed overnight in 4% (w/v) buffered paraformaldehyde followed by immersion in 30% (w/v) sucrose solutions in 1×PBS for cryoprotection until the tissue was fully infiltrated. Samples were embedded in optimal cutting temperature (OCT) medium and frozen by placing in a glass container with methyl butane kept on dry ice. Samples were stored at −80°C until sectioned coronally at a 20 μm thickness with a cryostat (CryoStar™ NX70; Thermo Fisher Scientific).

Quantification of HRP extravasation

The tissue section was incubated in PBS buffer for 20 min at room temperature before use. The tissue sampling regions were approximately −1.65 mm Bregma (four sections per animal, $n=4$ animals per group). For HRP analysis, freshly prepared DAB substrate solution (200 μL) was added to the tissue and incubated for 10 min at room temperature. Slides were then washed in deionized water three times (2 min each) and coverslips were mounted after adding a drop of aqueous mounting media. Sections were imaged using Slide Scanner (PathScan Enabler IV; Meyer Instruments, TX). Region of interest of dimension 5.2×2.5 mm was selected around the injury penumbra, including the cortical and the hippocampus regions. The region of interest (ROI) images were then analyzed using ImageJ software (National Institute of Health, Bethesda, MD) to obtain the total number of positive pixels per ROI.

Quantification of NP accumulation

For NP analysis, similar to HRP analysis, slides containing the frozen sections were incubated at room temperature for 20 min in 1×PBS to rehydrate the tissue and remove OCT compound. Coverslips were mounted on the section after adding one drop of fluorescent mounting media (Vectashield). The tissue sampling regions were approximately −1.65 mm Bregma, and the ipsilateral cortex (four sections per animal; $n=4$) and contralateral cortex (two sections per animal, $n=4$) were imaged with the conventional epi-fluorescence microscopy at 10× objective. All images were taken at the same exposure time and consistent acquisition settings.

Similar to HRP analysis, a region of interest 5.2×2.5 mm was selected around the injury penumbra, including the cortical and the hippocampus regions. The ROI images were then analyzed using ImageJ software (National Institute of

Health). A threshold was set using images from sham cohort tissues to remove background noise and was kept constant for ipsilateral and contralateral image analysis. The thresholded images were used to obtain the total number of positive pixels per ROI.

Two-photon microscopy: cranial window placement and imaging

Transgenic mice (female and male) underwent the CCI injury induction as described above. Based on the imaging time points (immediately after the injury or at 24 h, 3 days, or 7 days postinjury), anesthetized animals received intravenous NP injections (30 mg/kg b.w., 50 μL; retro-orbital). Following the injection, a cranial window was placed for imaging. The cranial window protocol is modified from a previously published protocol.[34,35] Briefly, the craniectomy/injury region was cleaned using saline, and gel foam soaked in saline was applied to stop any bleeding (if any). The region around the craniectomy was dried using a cotton swab. After ensuring no bleeding, a 5-mm-diameter glass coverslip was gently placed on the brain tissue, centered at −2 mm bregma and 2 mm lateral midline (Supplementary Fig. S6a, b).

The glass coverslip was sealed using dental cement to secure it and to create a well for the water-immersion objective. One cohort of control sham animals were used to establish baseline NP extravasation. These sham animals were anesthetized, injected with NPs, then subjected to craniectomy (4 mm), and cranial window placement according to the aforementioned protocol.

For imaging, animals remained under anesthesia (isoflurane) and were mounted on a microscope adaptable animal holding frame. Animals were placed on the mount using ear bars to stabilize their heads, and a two-photon laser scanning microscope (FVMPE-RS) from Olympus (Tokyo, Japan) was used. A water immersion 25× objective lens (NA = 1.05) was used to image NPs present inside the cerebral microvessels and diffuse the NP signal indicating NP extravasation outside of the blood vessels. Twelve-bit images of 512×512 pixels (0.509×0.509 mm in the x-y plane) were obtained with a galvano scanner via one-way scan direction and sampling speed of 4.0 μs/pixel. The excitation wavelength of 920 nm was used for the red channel and green channel with ∼15% laser transmissivity.

Imaging was completed at a depth ∼75–80 μm below from the coverslip to avoid any artifact related to superficial bleeds that arise during coverslip placement. Animals were imaged for a maximum of 3 h under anesthesia (isoflurane). After two-photon imaging was completed, while animals were still under anesthesia, HRP (83 mg/kg of b.w. injection volume of 25 μL) was injected via retro-orbital 10 min before sacrifice. Animals were perfused using the protocol explained above.

Magnetic resonance imaging lesion volume analysis

MRI was performed longitudinally at 3 h, 24 h, 3–4 days (3 days for male cohort and 4 days for female cohort), and 7 days postinjury using ParaVision software on a Bruker BioSpin 7T system (Bruker BioSpin Corp., Billerica, MA). A volume transmitter coil (72 mm) was used in conjunction with a mouse brain surface coil for signal detection. Animals were placed at a prone position on a nonmagnetic holder with the teeth bar as an aid to fix the head position. During image acquisition, anesthesia was maintained using isoflurane (1.5%) while the body temperature was maintained at 37°C using a circulating water blanket. Respiration and rectal temperature were monitored using SAI system. T2-weighted scans were acquired using a fast-spin echo sequence (TR/TE/ETL = 4000 ms/60 ms/8, resolution of 0.1× 0.1×0.5 mm, 30 slices).

The T2-weighted scans were then imported into ImageJ for lesion volume analysis. For each scan, freehand ROIs were drawn around the injury for each slice. The ROI/injury was determined by visually evaluating the area of signal hyperintensity around the location where the cortical impact occurred. The lesion volume was computed for a scan by summing the area of the ROIs of each slice of that scan in terms of the number of voxels. This volume was found for each animal for each time point.

Immunohistochemical staining, imaging, and quantification

Four tissue sections per animal were analyzed. Tissue sections were washed four times for 15 min between all stains. Initially, sections were blocked for 1 h using 8% horse serum and 0.2% Triton X in 1×PBS. Sections were incubated overnight at 4°C in 1:500 goat anti-GFAP, 2% horse serum, and 0.1% Triton X in 1×PBS. Slides were then incubated for 2 h in 1:500 donkey anti-goat 647 secondary with 2% horse serum in 1×PBS in dark. Finally, slides were stained with 4′,6-diamidino-2-phenylindole (DAPI), mounted with Vectashield, and sealed with nail polish. Slides were imaged at 20× on the Zeiss LSM800 laser scanning confocal microscope.

The region of interest for imaging was selected at the penumbra region of the injury site, ∼200–500 μm away from the lesion site to avoid the necrosis region. DAPI and glial fibrillary acidic protein (GFAP) image acquisition settings were held constant. Images were taken around the injury and on the contralateral hemisphere. The percent area was calculated using ImageJ. A threshold was set using tissues from secondary control images to remove background noise and was kept constant for ipsilateral and contralateral images. The thresholded images (ipsilateral and contralateral) were quantified using analyzed particles. The percent area result was then averaged per animal.

Statistics

Statistical analyses were conducted in GraphPad Prism 5.0 (GraphPad Software, Inc., La Jolla, CA). For HRP, NP, and GFAP analysis, an ordinary two-way ANOVA was conducted to analyze female and male cohorts individually. If there was a significant main effect of hemisphere (ipsilateral vs. contralateral) and/or significant interaction effect, the two-way ANOVA was followed by a *post hoc* Bonferroni's multiple comparison test.

To evaluate the sex dependence for HRP, NP, and GFAP analysis, an ordinary two-way ANOVA was conducted using ipsilateral hemispheres of female and male cohorts. If there was a significant main effect of sex (female vs. male) and/or significant interaction effect, the two-way ANOVA was followed by a *post hoc* Bonferroni's multiple comparison test. For MRI analysis, a two-way ANOVA with replication was conducted to analyze the effect of both time and sex on injury lesion volume. If there was a significant main

effect of sex (female vs. male) and/or significant interaction effect, the two-way ANOVA was followed by a *post hoc* Bonferroni's multiple comparison test.

Results

The lateral CCI imparts an injury directly to the fronto-parietal cortex generating a cortical lesion ipsilateral to the impact with no direct damage to the contralateral hemisphere. Brain injury may lead to a transient BBB disruption that could potentially allow therapeutic delivery to the injured brain regions. See Supplementary Figure S1 for experimental design/time line. The focus of this study was threefold: (1) to investigate delivery dynamics of macromolecules and NPs, (2) to determine acute and subacute temporal delivery profiles, and (3) to examine sex dependence for delivery of these therapeutic agents.

Extravasation of intravenously injected macromolecular tracer (HRP) after focal brain injury

To examine the potential delivery of the macromolecules, a large MW tracer, HRP (40 kDa), was used as a surrogate.[18,21,36] Each cohort received intravenous HRP injection 10 min before sacrifice at 3 h, 24 h, 3 days, and 7 days following CCI injury. The HRP extravasation was analyzed at the core of the injury (approximately −1.65 mm Bregma). The extravasation of HRP at the 3-h, 24-h, and 3-day time points was restricted to the primary injury region (Fig. 1a). We observed no HRP staining in the contralateral hemisphere for any time point postinjury (Supplementary Fig. S2). Two-way ANOVA revealed a significant main effect of both hemisphere ($p < 0.0001$) and time ($p < 0.0001$) on HRP levels for both the sexes (Fig. 1b, c, respectively); a significant interaction between hemisphere and time was also discovered ($p < 0.0001$) (Supplementary Table S1 for statistical details).

Pairwise analysis of extravasation of HRP in both the sexes showed markedly higher levels of HRP stain at 3 h, 24 h, and 3 days postinjury compared with their respective contralateral hemispheres. At 7 days postinjury, the HRP staining in the ipsilateral location for both the sexes was minimal and not significant compared with their contralateral hemisphere. At 3 h postinjury for both the sexes, HRP staining was significantly different than the 24-h postinjury ipsilateral hemisphere. Interestingly, the male 3-day (ipsilateral) cohort showed a significant increase ($\sim$150% increase) in HRP staining relative to the 24-h male ipsilateral group.

A two-way ANOVA revealed a significant main effect for both sex ($p = 0.0004$) and time ($p < 0.0001$) on ipsilateral HRP levels (Fig. 1d); the interaction between sex and time was also significant ($p = 0.0119$) (Supplementary Table S1 for statistical details). Specifically, at 24 h postinjury, there was significantly increased HRP staining in females compared (3$\times$higher) with their male counterparts ($p = 0.0002$). This observation supported the previously reported biphasic BBB disruption pattern for male cohorts.[6,17] However, more intriguingly, the females exhibited consistent HRP staining levels at both 24 h and 3 days postinjury, not following a biphasic response.

Taken together, the extravasation of the macromolecular tracer was observed acutely (3 and 24 h) and subacutely (3 days) postinjury, demonstrating a potential for delayed therapeutic macromolecule delivery. Furthermore, more strikingly, the macromolecular tracer delivery was sex dependent, where only the males showed a biphasic pattern.

Accumulation of intravenously injected NPs after focal brain injury

To examine the potential NP delivery at acute and subacute time points and the sex dependence for delivery after brain injury, we used fluorescent PEGylated 40 nm polystyrene NPs (see Supplementary Fig. S3 for NP characterization). Each cohort received an intravenous injection of the NPs 3 h before sacrifice (see Supplementary Fig. S4 for biodistribution data). Mirroring HRP analysis, the area of NP accumulation was quantified at the core of the injury (approximately −1.65 mm Bregma) via the epi-fluorescence microscope. NP accumulation was restricted to the primary injury region (Fig. 2a), similar to the HRP staining. We observed no detectable NP accumulation in the contralateral hemisphere for any time point postinjury (Supplementary Fig. S5).

Briefly, we found significant NP delivery for females acutely at 3 and 24 h and subacutely at 3 days postinjury. However, for males, the NP accumulation was significantly increased in the ipsilateral hemisphere compared with the contralateral hemisphere only at 3 h for acute delivery and at 3 days for subacute delivery. Moreover, there was a significantly higher NP accumulation at 24 h postinjury in females compared with males (Fig. 2b; 2.5$\times$higher). These results trended similar to HRP extravasation.

Two-way ANOVA showed a significant main effect for both the hemisphere ($p < 0.0001$) and time ($p < 0.0001$) on HRP extravasation in both female (Fig. 2b) and male cohorts (Fig. 2c); the interaction between hemisphere and time was also significant ($p < 0.0001$) (Supplementary Table S2 for statistical details). For the female cohort, the pairwise analysis revealed significantly increased NP accumulation ipsilaterally at 3 h ($p < 0.0001$), 24 h ($p = 0.0004$), and 3 days ($p = 0.002$) compared with their respective contralateral hemisphere. For the male cohort, a significant increase in NP accumulation was detected at 3 h ($p < 0.0001$) and 3 days ($p = 0.0052$), whereas the effect was marginal at 24 h ($p = 0.0508$) postinjury compared with their respective contralateral location. At 7 days postinjury, both female ($p > 0.9999$) and male cohorts ($p > 0.9999$) did not show significant NP accumulation compared with their respective contralateral location.

The 3 h ipsilateral NP accumulation was maximal for both female ($p < 0.0001$, $\sim$150% increase) and male ($p < 0.0001$, $\sim$500% increase) compared with all other time points (24 h, 3 days, and 7 days) in the ipsilateral hemisphere. Similar to HRP staining, there was no significant difference in NP accumulation between 24 h and 3 days in the ipsilateral hemisphere in the female ($p = 0.9672$) cohort. However, in contrast to the HRP staining, there was no significant difference in NP accumulation in males at 24 h and 3 days in the ipsilateral hemisphere ($p = 0.7509$).

To investigate the sex dependence for NP delivery, we used two-way ANOVA to compare the female and male ipsilateral hemispheres across time points. Overall, the analysis revealed a significant interaction effect between sex and time ($p = 0.0087$) with a significant main effect of time on NP accumulation ($p < 0.0001$), but no main effect of sex on NP accumulation ($p = 0.2402$) (Supplementary Table S2 for statistical details). A *post hoc* pairwise analysis at 24 h

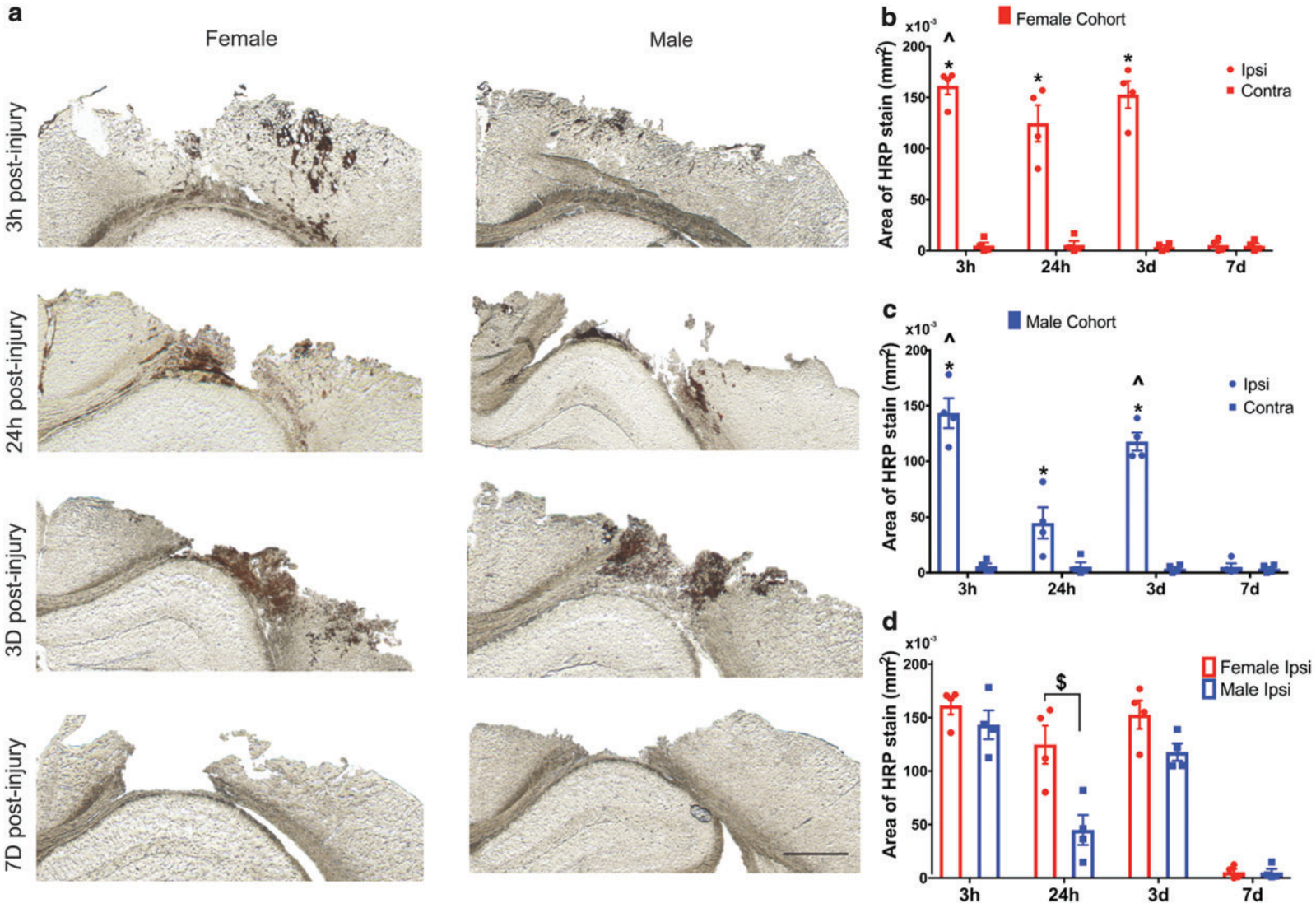

FIG. 1. Macromolecular tracer (HRP) extravasation after CCI: **(a)** Ipsilateral hemisphere: Representative images of HRP extravasation (*dark brown* staining) at 3 h, 24 h, 3 days, and 7 days post-CCI. The *first column* shows the HRP response in the female cohort and the *second column* in males. Scale bar = 1 mm. **(b, c)** Sex dependence of HRP extravasation: Extravasation of HRP in the female cohort **(a)** and male cohort **(b)** at different time points postinjury. **(d)** Quantification of HRP stain in the ipsilateral hemisphere of female and male cohorts across different time points. $^{*}p < 0.05$ compared to their respective contralateral hemisphere and 7 days ipsilateral hemisphere, two-way ANOVA, Bonferroni's multiple comparisons. $^{\wedge}p < 0.05$ compared to 24-h ipsilateral hemisphere, $^{\$}p < 0.05$ compared to male 24-h ipsilateral hemisphere, two-way ANOVA, Bonferroni's multiple comparisons. Error bars represent standard error of mean, $n = 4$. CCI, controlled cortical impact; HRP, horseradish peroxidase. Color images are available online.

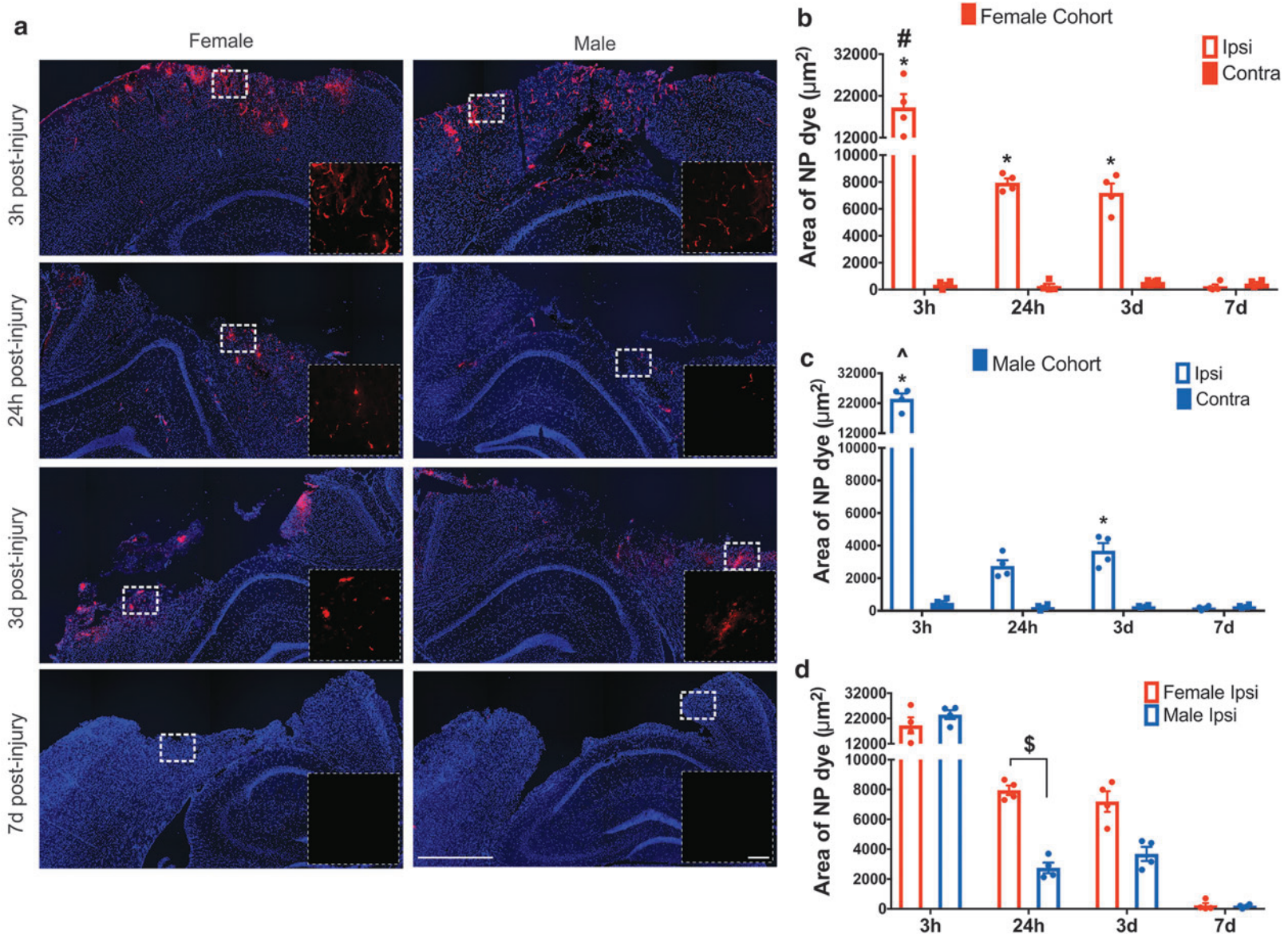

FIG. 2. **(a)** NP accumulation after TBI in the ipsilateral hemisphere: Representative images of NP extravasation at 3 h, 24 h, 3 days, and 7 days post-CCI. The *first column* shows the NP accumulation in the female cohort and the *second column* in males. The *inset* image is the enlarged view of the *white dotted box* in the main image. Main image scale bar = 750 μm, *inset* image scale bar = 100 μm. **(b, c)** NP accumulation in female and male cohort: Accumulation of NP in the female cohort **(b)** and male cohort **(c)** at different time points postinjury. $^{*}p < 0.05$ compared to their respective contralateral hemisphere and 7-day ipsilateral, two-way ANOVA, Bonferroni's multiple comparisons. $^{\#}p < 0.05$ compared to 24-h and 3-day ipsilateral hemisphere. $^{\wedge}p < 0.05$ compared to 24-h ipsilateral hemisphere, $^{\$}p < 0.05$ compared to male 24-h ipsilateral hemisphere, two-way ANOVA, Bonferroni's multiple comparisons. Error bars represent standard error of mean, $n = 4$. **(d)** Quantification of NP accumulation in ipsilateral hemisphere of female and male cohorts across different time points. NP, nanoparticle; TBI, traumatic brain injury. Color images are available online.

showed a significantly increased NP accumulation in females compared with males ($p = 0.0437$), comparable to the HRP extravasation profile.

Overall, we found significant NP accumulation in the ipsilateral hemisphere at acute and subacute time points in both female (3 h, 24 h, and 3 days) and male (3 h and 3 days) cohorts compared with the contralateral hemisphere. Furthermore, the ipsilateral hemisphere of the females showed significantly increased NP accumulation at 24 h postinjury compared with the male cohort.

Intravital two-photon microscopy imaging after intravenous injection of NP

The histological assessment demonstrated significant NP accumulation within the injury penumbra over the first 3 days after injury. However, tracking NP dynamics in postmortem, perfused tissue sections is difficult, and artifacts related to perfusion-fixation itself may alter NP localization. Therefore, we used intravital two-photon microscopic imaging for up to 3 h after NP injection for each postinjury cohort to decipher intravascular NP deposition versus extravasation into the parenchyma. The main advantage of two-photon microscopy imaging is the powerful resolution to visualize single cortical vessels and their surrounding cells after CCI. Moreover, we were able to image the dynamics of NP localization in the deep cortical regions ($\sim 75\,\mu m$) postinjury in live tissue *in vivo* (Supplementary Videos S1, S2, and S3, and Fig. 3).

A combination of exogenous (via fluorescent NPs) and endogenous (via CX3CR1-GFP$^+$) fluorescent labels was used to visualize the vascular and extravascular tissue. Transgenic mice with GFP tagged with CX3CR1 were used for direct visualization of microglia/macrophage cells present within the parenchyma, prominent inflammatory players following TBI. A cranial window technique was used to enable imaging of GFP$^+$ microglia cells and track the NPs with minimal perturbation to the normal physiological functions in live animals.

For each animal, a single two-photon video recording session was conducted for a maximum of 3 h after NP injection within the injury penumbra, with as a minimum, one scan per hour lasting at least 5 min per scan. Overall, at least three different locations were imaged focusing on regions with identifiable, semi-intact blood vessels (Supplementary Fig. S6). Representative still images in Figure 3a, and Supplementary Videos S1 and S2 show NP (in red) and the CX3CR1-GFP$^+$ cells (microglia/macrophage; green). In the sham animals (Supplementary Video S3), we observed intact large blood vessels with the NP fluorescence and no NP extravasation, surrounded by ramified microglia (Fig. 3b). In addition, we observed activated microglia with amoeboid

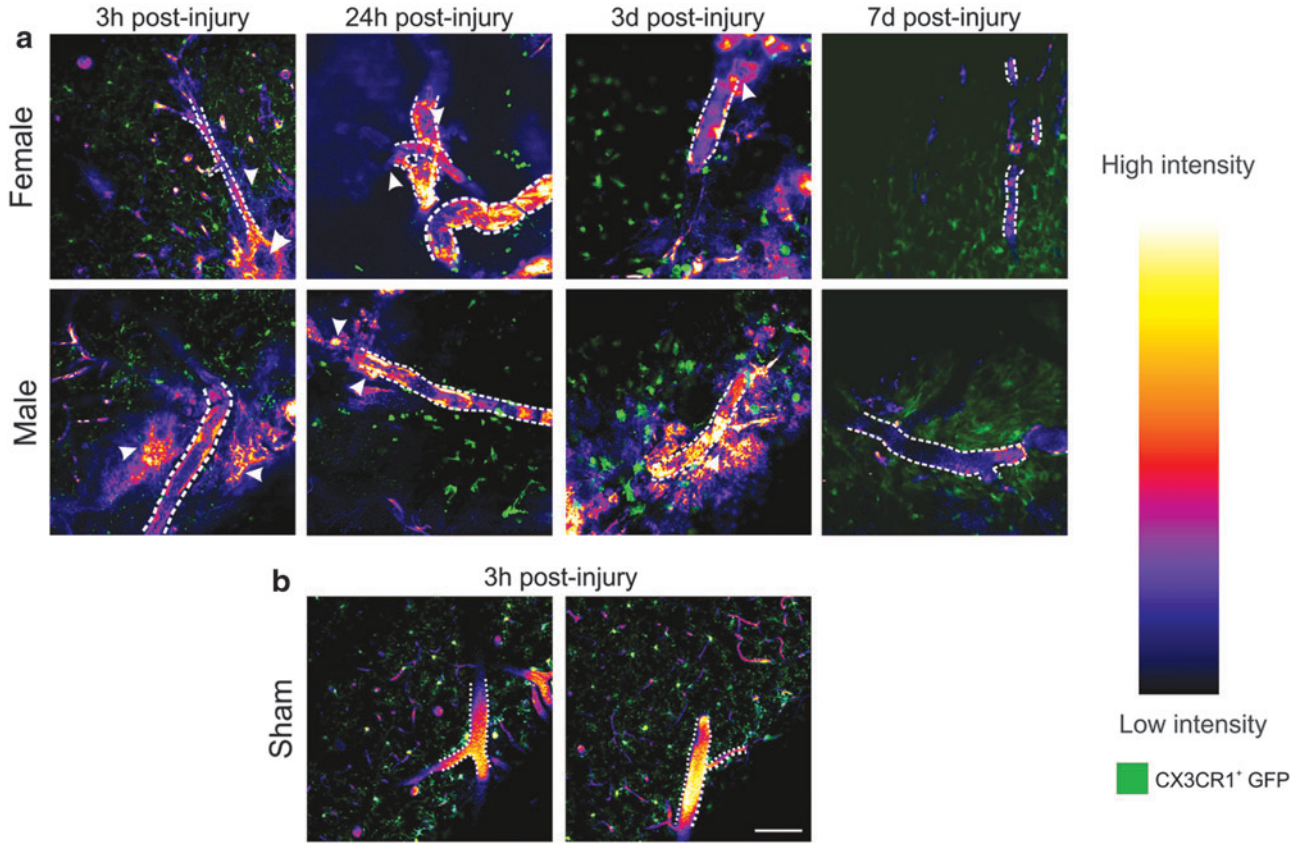

FIG. 3. Two-photon intravital microscopy in the cerebral cortex after CCI. **(a)** Representative images of intravenously injected NPs (intensity map) acquired from the peri-injury zone of the cortex at 3 h, 24 h, 3 days, and 7 days post-CCI in CX3CR1-GFP$^+$ transgenic mice (*green*) (blood vessels are denoted by a *dotted white* outline). Extravasation of NPs was evident in both male and female mice at 3 h, 24 h, and 3 days as diffuse labeling around the blood vessel (*white arrowheads*), shown here using a heatmap of grayscale intensity values on the *right*. At 7 days postinjury, there was no visible NP extravasation. **(b)** No extravasation or dispersed NP signal was observed in sham injury cohort animals. Supplementary Figure S6 shows the cranial window setup and the imaging location. Scale bar = 100 μm. Color images are available online.

morphology at 24 h and 3 days postinjury that corroborates previous studies.[37,38] We did not observe any detectable NP intensity within the extravascular tissue at 7 days postinjury in either sex.

Injury lesion volume analysis: MRI analysis

MR images were used to quantify lesion volume size for sex comparison across the different time points (Fig. 4). A longitudinal time series of 1-mm-thick anatomically coronal T2-weighted spin-echo images (female, Fig. 4a; male, Fig 4b) show the evolution of the injury and lesion volume over time. It must be noted that the male cohort was imaged at 3 h, 24 h, 3 days, and 7 days, whereas the female cohort was imaged at 3 h, 24 h, 4 days, and 7 days postinjury. The MR scans at 3 and 24 h show a typical signal hyperintensity at and around the injury site, characteristically interpreted as acute edema.[39,40] By 3–4 days, this hyperintensity is reduced, suggesting that the acute edema is resolving.[39,40] At 7 days, there is typically an area of signal hyperintensity at the center of the injury region, usually interpreted as an area where tissue has been lost and replaced by fluid.[39,40]

Two-way ANOVA showed no significant interaction between sex and time ($p = 0.8084$); yet, a significant main effect of both sex ($p = 0.0017$) and time ($p = 0.0001$) on lesion volume was identified (Supplementary Table S3 for statistical details). Pairwise *post hoc* analysis showed no significant differences between the sexes for any time point. While these analyses indicate an overall main effect of sex on lesion size (i.e., females trended toward larger lesion volumes than males overall), within each time point, no significant differences existed between sexes.

Neuroglial response: immunohistochemical analysis of neuroglial response

Neuroglial response in females and males in the ipsilateral and contralateral cortex was evaluated based on the level of reactive astrocytosis using GFAP immunostaining. The representative images of the ipsilateral hemisphere are shown in Figure 5a, and the contralateral images are shown in Supplementary Figure S7. Two-way ANOVA showed a significant interaction between location (hemisphere) and time ($p < 0.0026$, $p < 0.0002$) and also a significant main effect for both hemisphere ($p \leq 0.0002$, $p < 0.0001$) and time on GFAP immunostaining ($p < 0.0047$,

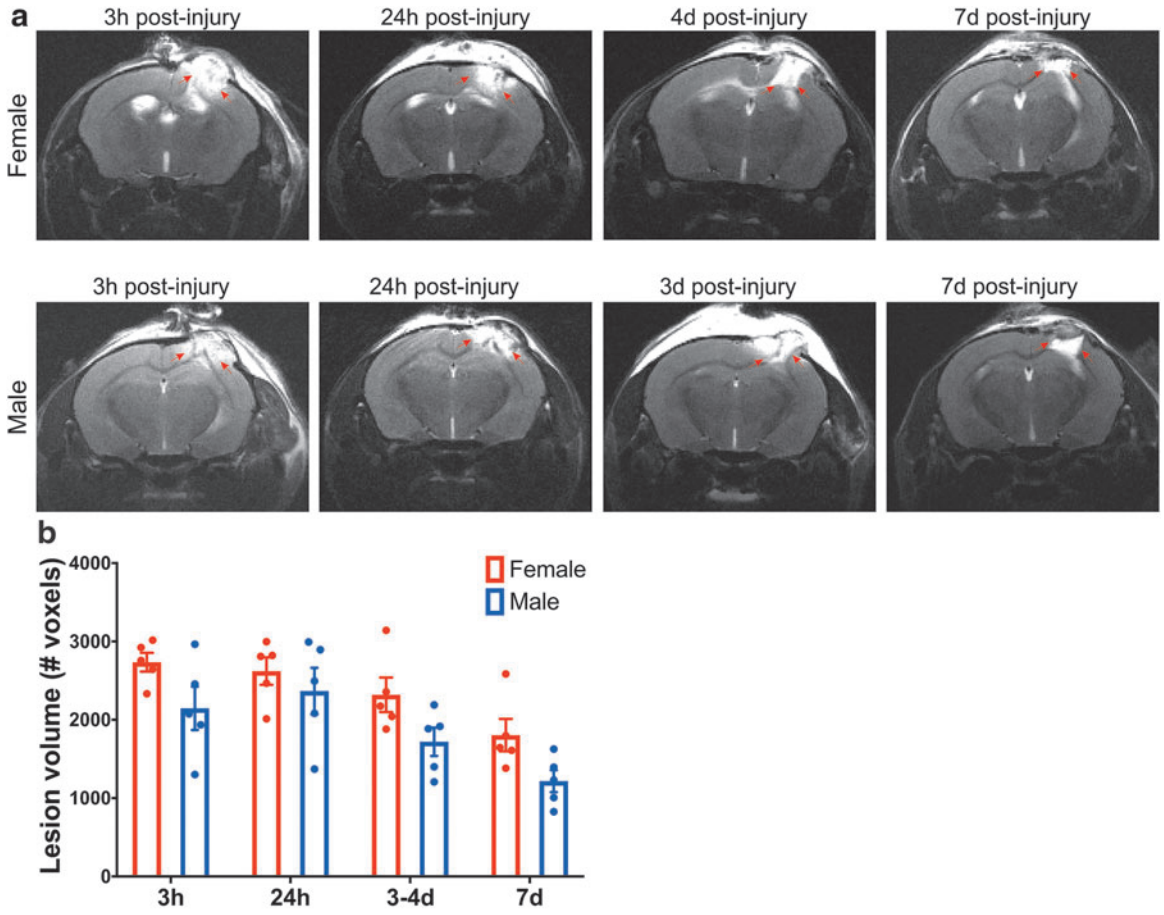

FIG. 4. **(a)** Longitudinal *in vivo* T2-weighted MRI reveals changes in the cerebral cortex (*right hemisphere*) after CCI injury. A longitudinal cohort of female and male mice were repeatedly scanned at 3 h, 24 h, 3 days (male) or 4 days (female), and 7 days postinjury. *Red arrows* highlight the hyperintensity at and around the injury site. **(b)** Quantification of lesion volume T2-weighted scans acquired using a fast-spin echo sequence. Two-way ANOVA, *post hoc* Bonferroni's analysis of the lesion volume comparison between sexes showed no significant difference at 3 h, 24 h, 3–4 days, and 7 days postinjury. Mean ± SEM, $n = 5$. MRI, magnetic resonance imaging; SEM, standard error of the mean. Color images are available online.

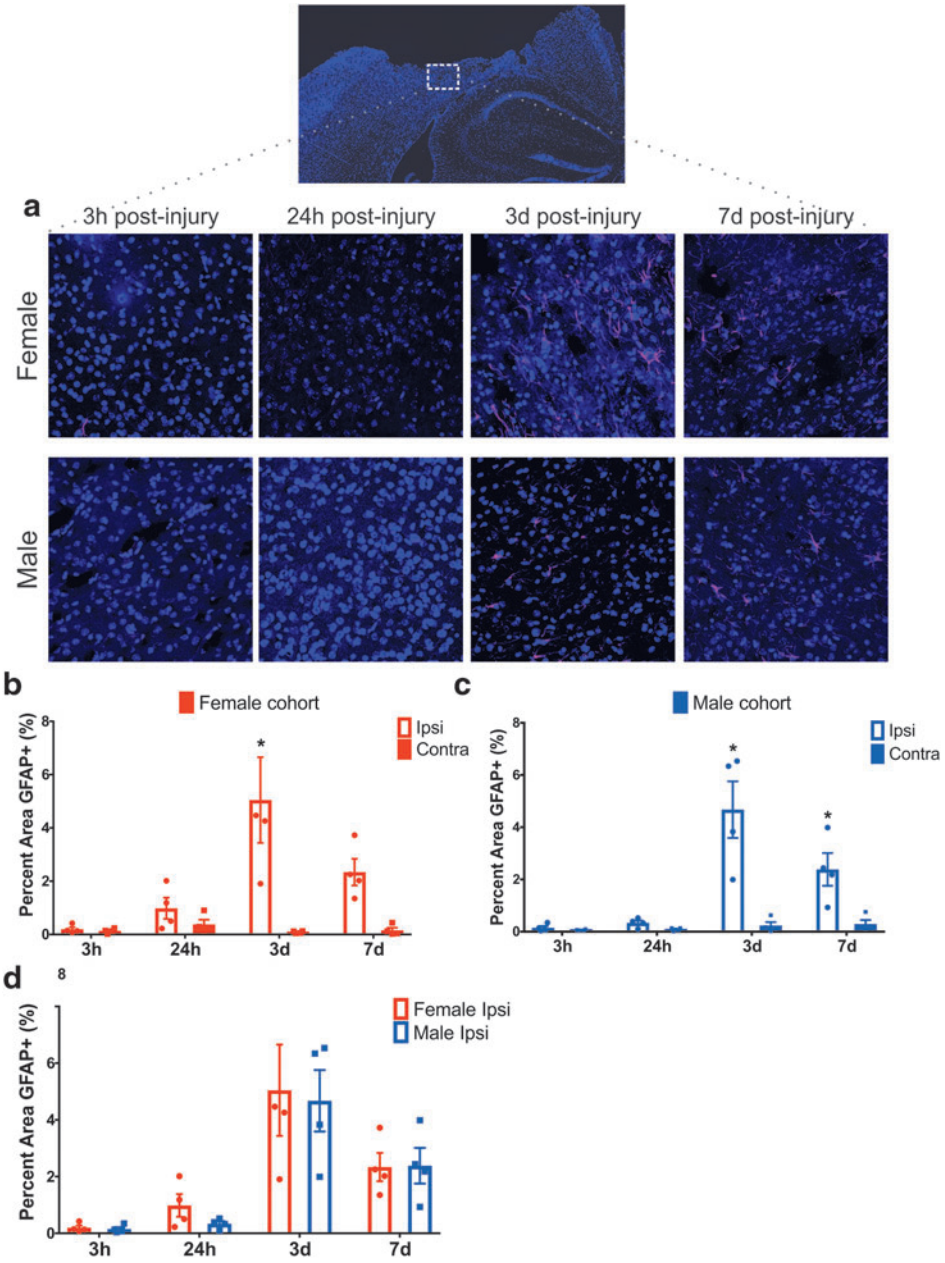

FIG. 5. **(a)** Representative images of anti-GFAP staining within the cortical injury penumbra show progressive astrocyte reactivity at 3 h, 24 h, 3 days, and 7 days postinjury in both females and males. **(b, c)** Quantification of GFAP staining in the ipsilateral cortex in female cohort **(b)** and male cohort **(c)** at different time points postinjury. **(d)** Quantification of GFAP staining in the ipsilateral hemisphere of female and male cohorts across different time points, found no difference between sexes at 3 h, 24 h, 3 days, and 7 days postinjury. Two-way ANOVA mean ± SEM, $n = 4$ per group. GFAP, glial fibrillary acidic protein. Color images are available online.

$p < 0.0001$), respectively, for female (Fig. 5b) and male cohorts (Fig. 5c) (Supplementary Table S4 for statistical details). We observed minimal GFAP expression at 3 and 24 h postinjury for both the sexes. For the female cohort, pairwise analysis revealed significantly increased GFAP staining ipsilaterally at 3 days ($p < 0.0001$) postinjury compared with the contralateral hemisphere.

For the male cohort, a significant increase in GFAP staining was detected at 3 days ($p < 0.0001$) and 7 days ($p = 0.0127$) postinjury compared with their respective contralateral location. To investigate the sex dependence, a two-way ANOVA revealed no significant interaction between sex and time nor a main effect of sex. Time was identified as a significant main effect on GFAP immunostaining levels ($p < 0.0001$) (Fig. 5d). Taken together, the results show no significant sex difference in GFAP expression at any time point postinjury.

Discussion and Conclusion

The BBB is a unique element of the brain that regulates molecular transport from the bloodstream to the brain parenchyma. Although the BBB disruption after TBI is thought to be detrimental, such opening may provide an opportunity for the delivery of drugs and therapeutics via NPs. To fully utilize the window of opportunity of BBB opening after TBI, a thorough assessment of the temporal resolution and the sex dependence of macromolecule for NP accumulation via the BBB was warranted. In this study, we directly address the critical gap using a focal TBI mouse model and intravenously injecting macromolecular tracer and PEGylated polystyrene NPs.

The four key insights include the following. (1) Significant macromolecular tracer extravasation occurred at

acute (3 h, 24 h) and subacute (3 days) postinjury time points after focal brain injury regardless of the sex; (2) significant NP accumulation was observed acutely (3 h, 24 h in females and 3 h in males) and subacutely (3 days) after brain injury; (3) sex-dependent effects were observed with a biphasic pattern in males showing a significant accumulation of the macromolecular tracer/NP at acute (3 h) and subacute (3 days) time points, but a significant decrease at 24 h postinjury. In contrast, females showed a significant decrease at 24 h but continued to display significant accumulation within the first 3 days postinjury; (4) no sex differences were observed in the neuroglial response (GFAP) and while there was an overall main effect of sex on brain lesion volume (MRI analysis), no significant pairwise differences were observed at each time point.

Placing our data in context with prior studies that investigate differential sex responses to TBI, the following points are critical to consider. At our most acute (3 h) time point postinjury, we observed a peak accumulation of HRP and NP in both sexes with no significant sex differences. The CCI model consistently produces cortical damage, including tearing of the dura, parenchyma, and severe vascular disruption directly at the site of impact.[6,17,41,42] Our findings of no sex differences 3 h postinjury in HRP and NP accumulation support mechanical disruption of the BBB from the primary impact. Comparing our data with previous studies using a diffuse TBI model, minimal BBB opening in intact (normal cycling) females was reported compared with significant BBB disruption in males at 5 h postinjury.[28,43]

At 24 h postinjury, a sex-dependent BBB disruption emerged. Specifically, the females displayed a robust HRP/NP accumulation that was nearly 2.5–3 × than their male counterparts. Although previous reports using a different injury model[29] and endogenous marker[30] reported no sex differences in the BBB permeability at 24 h postinjury. The contrast between studies highlights the importance of considering injury phenotype (diffuse vs. focal) and molecular tracer when comparing BBB disruption profiles. Notably, we designed our study to capture the dynamics of macromolecule and NP extravasation at distinct phases postinjury by intravenously injecting exogenous markers of NP (3 h) and HRP (10 min) before sacrifice and perfusion at distinct time points postinjury. Moreover, the males showed a biphasic trend with a significant decrease in HRP/NP at 24 h compared with 3 h and 3 days postinjury, in alignment with previous seminal studies in male rodents using the large MW tracer.[17,44]

At subacute (3 days) time point, we observed significant macromolecular tracer and NP accumulation in both the sexes compared with their respective contralateral region. Delayed BBB disruption is mainly associated with the secondary injury that follows the primary injury, although the mechanism(s) have not been clearly elucidated.[7,45] Evidence suggests increased paracellular permeability due to disruption of tight junction complexes and integrity of the basement membrane as a dominant mechanism.[7,45] The pathophysiological processes such as oxidative stress and coagulation cascade initiate glial cell activation and alter their interaction with the cerebrovascular endothelial cells potentially further contributing to BBB dysfunction.[7,45,46] Taken together, to the best of our knowledge, this is the first report showing that the BBB disruption is sex dependent for macromolecule and NP extravasation.

One of the key findings of our study is the differential sex response at 24 h postinjury between the macromolecular tracer (3 × higher) and NP accumulation (~2.5 × higher) in females compared with males. These results were obtained from cohorts with no significant sex-dependent variations in astrogliosis and lesion volume. As such, this observation of the lack of sex-dependent differences in GFAP expression and lesion volume, but a significant sex-dependent difference in the BBB disruption, has a few caveats and needs to be interpreted cautiously. First, it must be noted that we only probed four time points (3 h, 24 h, 3 days, and 7 days) across the injury progression, and it could be possible that the sex-dependent differences in the GFAP expression and/or lesion volume were not captured at the time points we have investigated. Second, we used normal (intact gonads) mice, and female mice were at random estrous cycle, and thus, we are unable to distinguish the impact of specific sex hormone on BBB permeability.

Previous studies have suggested female sex to be a risk factor for greater BBB permeability and ovarian hormones to be detrimental for the BBB in some conditions.[47–49] The impact of sex hormone on BBB might be critical to explain our observation of sex-dependent differences in BBB permeability with lack of significant sex-dependent difference in injury progression, and future studies are necessary. Although numerous preclinical TBI studies report a female neuroprotective effect implicating estrogen- or progesterone-mediated mechanisms,[50–52] a few studies report no impact of sex on the outcome.[53,54] In contrast, clinical studies cite worse outcomes for females compared with males.[55,56] Our study design mirrored prior work that indicated that the phase of the estrous cycle at the time of injury does not significantly affect functional outcomes following TBI.[57] Yet, future studies are warranted as a study by Maghool *et al.* in rats reported that females in the proestrus phase are less vulnerable to brain injury compared with females in the nonproestrus phase as measured by levels of brain edema and intracranial pressure.[58]

Furthermore, it is important to recognize that a TBI event may alter subsequent sex hormone levels thereby affecting estrous cycles acutely after injury. A preclinical rat study shows evidence that TBI leads to disruption of the estrous cycle with significantly reduced 17β-estradiol (E2) hormone levels[59] and spatial memory impairment compared with the sham group. Similarly, clinical studies indicate that TBI affects the circulating serum hormone levels in both females and males.[57,60] In females, testosterone increased with modest/no increase in estrogens.[57] In males, estrogen increases with a decrease in testosterone.[60] Therefore, comprehensive studies to understand the specific mechanism that drives the pathophysiological changes and the role of sex hormones in neuroprotection and BBB breakdown after TBI are warranted.

In conclusion, to the best of our knowledge, we report for the first time that (1) female mice exhibit a robust macromolecular tracer (3 × higher) and NP accumulation (2.5 × higher) at the 24-h time point after focal TBI compared with male mice, primarily due to sex differences in BBB permeability in response to the injury and (2) we demonstrate the ability to delivery macromolecules and NPs at the subacute time point (3 days) after focal injury in both the sexes.

The implications of our novel findings are far-reaching for personalized and precision medicine. The sex differences

in macromolecular and NP extravasation may impact the pharmacokinetics and pharmacodynamics of the therapeutic delivery after brain injury. Moreover, the sex-based differences in extravasation may influence the drug dose, drug concentration, and desired bioavailability near the injured brain tissue between female and male subjects. Therefore, a better understanding of the sex differences is essential to appropriately conduct a risk assessment and to design safe and effective treatments. Future studies to elucidate the underlying hormonal and sex-related differences for variable BBB permeability are warranted.

Acknowledgments

Authors thank Katherine R. Giordano for assisting in breeding the transgenic animals and Chen Wu for helping with perfusions of the transgenic animals. They thank Dr. Shenfeng Qiu for lending the animal mount for two-photon microscope imaging study. The authors thank Jordan Todd and Kyle Offenbacher for their technical assistance. They thank the Barrow-Arizona State University Center for Preclinical Imaging for the use of MRI and IVIS spectrum. They also thank Xiaowei Zhang for performing the MRI. They thank Dr. Racheal Sirianni for the use of dynamic light scattering device. The authors thank Brian Cherry and the Magnetic Resonance Research Center at Arizona State University for NMR analysis. They thank the Keck imaging facility for the fluorescence spectrophotometer use.

Disclosure Statement

No competing financial interests exist.

Funding Information

This study was supported by the FLINN Foundation (S.E.S., V.D.K., J.L., P.D.A.), NIH (R00NS076661 and R01NS097537 to J.M.N.; 1DP2HD084067 to S.E.S.), and Arizona State University Graduate College Completion Fellowship (V.N.B.).

Supplementary Material

Supplementary Data
Supplementary Table S1
Supplementary Table S2
Supplementary Table S3
Supplementary Table S4
Supplementary Figure S1
Supplementary Figure S2
Supplementary Figure S3
Supplementary Figure S4
Supplementary Figure S5
Supplementary Figure S6
Supplementary Figure S7
Supplementary Video S1
Supplementary Video S2
Supplementary Video S3

References

1. Pardridge, W.M. The blood-brain barrier: bottleneck in brain drug development. NeuroRX **2,** 3, 2005.
2. Banks, W.A. From blood–brain barrier to blood–brain interface: new opportunities for CNS drug delivery. Nat Rev Drug Discov **15,** 275, 2016.
3. Saunders, N.R., Habgood, M.D., Møllgård, K., and Dziegielewska, K.M. The biological significance of brain barrier mechanisms: help or hindrance in drug delivery to the central nervous system? F1000Res **5,** 313, 2016.
4. Gennarelli, T.A. The pathobiology of traumatic brain injury. Neuroscientist **3,** 73, 1997.
5. Davis, A.E. Mechanisms of traumatic brain injury: biomechanical, structural and cellular considerations. Crit Care Nurs Q **23,** 1, 2000.
6. Baldwin, S.A., Fugaccia, I., Brown, D.R., Brown, L.V., and Scheff, S.W. Blood-brain barrier breach following cortical contusion in the rat. J Neurosurg **85,** 476, 1996.
7. Shlosberg, D., Benifla, M., Kaufer, D., and Friedman, A. Blood–brain barrier breakdown as a therapeutic target in traumatic brain injury. Nat Rev Neurol **6,** 393, 2010.
8. Clond, M.A., Lee, B.-S., Yu, J.J., *et al.* Reactive oxygen species-activated nanoprodrug of ibuprofen for targeting traumatic brain injury in mice. PLoS One **8,** e61819, 2013.
9. Bharadwaj, V.N., Nguyen, D.T., Kodibagkar, V.D., and Stabenfeldt, S.E. Nanoparticle-based therapeutics for brain injury. Adv Healthc Mater **7,** 1700668, 2018.
10. Bickel, U., Yoshikawa, T., and Pardridge, W M. Delivery of peptides and proteins through the blood–brain barrier. Adv Drug Deliv Rev **46,** 247, 2001.
11. Petros, R.A., and DeSimone, J.M. Strategies in the design of nanoparticles for therapeutic applications. Nat Rev Drug Discov **9,** 615, 2010.
12. Masserini, M. Nanoparticles for brain drug delivery. ISRN Biochem **2013,** 1, 2013.
13. Fosgerau, K., and Hoffmann, T. Peptide therapeutics: current status and future directions. Drug Discov Today **20,** 122, 2015.
14. Usmani, S.S., Bedi, G., Samuel, J.S., *et al.* THPdb: database of FDA-approved peptide and protein therapeutics. PLoS One **12,** e0181748, 2017.
15. Bobo, D., Robinson, K.J., Islam, J., Thurecht, K.J., and Corrie, S.R. Nanoparticle-based medicines: a review of FDA-approved materials and clinical trials to date. Pharm Res **33,** 2373, 2016.
16. Ventola, C.L. Progress in nanomedicine: approved and investigational nanodrugs. P T **42,** 742, 2017.
17. Başkaya, M.K., Muralikrishna Rao, A., Doğan, A., Donaldson, D., and Dempsey, R.J. The biphasic opening of the blood–brain barrier in the cortex and hippocampus after traumatic brain injury in rats. Neurosci Lett **226,** 33, 1997.
18. Habgood, M.D., Bye, N., Dziegielewska, K.M., *et al.* Changes in blood-brain barrier permeability to large and small molecules following traumatic brain injury in mice: blood-brain barrier permeability following trauma. Eur J Neurosci **25,** 231, 2007.
19. Bharadwaj, V.N., Lifshitz, J., Adelson, P.D., Kodibagkar, V.D., and Stabenfeldt, S.E. Temporal assessment of nanoparticle accumulation after experimental brain injury: effect of particle size. Sci Rep **6,** 1, 2016.
20. Bharadwaj, V.N., Rowe, R.K., Harrison, J., *et al.* Blood–brain barrier disruption dictates nanoparticle accumulation following experimental brain injury. Nanomedicine **14,** 2155, 2018.
21. Tanno, H., Nockels, R.P., Pitts, L.H., and Noble, L.J. Breakdown of the blood–brain barrier after fluid percussive

brain injury in the rat. Part 1: distribution and time course of protein extravasation. J Neurotrauma **9,** 21, 1992.
22. Ping, X., Jiang, K., Lee, S.-Y., Cheng, J.-X., and Jin, X. PEG-PDLLA micelle treatment improves axonal function of the corpus callosum following traumatic brain injury. J Neurotrauma **31,** 1172, 2014.
23. Bailey, Z.S., Nilson, E., Bates, J.A., *et al.* Cerium oxide nanoparticles improve outcome after *in vitro* and *in vivo* mild traumatic brain injury. J Neurotrauma **37,** 1452, 2020.
24. Miller, H.A., Magsam, A.W., Tarudji, A.W., *et al.* Evaluating differential nanoparticle accumulation and retention kinetics in a mouse model of traumatic brain injury via Ktrans mapping with MRI. Sci Rep **9,** 16099, 2019.
25. Wu, P., Zhao, H., Gou, X., *et al.* Targeted delivery of polypeptide nanoparticle for treatment of traumatic brain injury. Int J Nanomedicine **14**, 4059, 2019.
26. Vagnerova, K., Koerner, I.P., and Hurn, P.D. Gender and the injured brain. Anesth Analg **107,** 201, 2008.
27. Caplan, H.W., Cox, C.S., and Bedi, S.S. Do microglia play a role in sex differences in TBI?: sex differences in TBI and microglia. J Neurosci Res **95,** 509, 2017.
28. O'Connor, C.A., Cernak, I., and Vink, R. The temporal profile of edema formation differs between male and female rats following diffuse traumatic brain injury. In: Hoff, J.T., Keep, R.F., Xi, G., and Hua, Y., eds. Brain Edema XIII, vol. 96. Vienna, Austria: Springer-Verlag, 2006, pp. 121–124.
29. Duvdevani, R., Roof, R.L., Fülöp, Z., Hoffman, S.W., and Stein, D.G. Blood–brain barrier breakdown and edema formation following frontal cortical contusion: does hormonal status play a role? J Neurotrauma **12,** 65, 1995.
30. Jullienne, A., Salehi, A., Affeldt, B., *et al.* Male and female mice exhibit divergent responses of the cortical vasculature to traumatic brain injury. J Neurotrauma **35,** 1646, 2018.
31. Nance, E.A., Woodworth, G.F., Sailor, K.A., *et al.* A dense poly(ethylene glycol) coating improves penetration of large polymeric nanoparticles within brain tissue. Sci Transl Med **4,** 149ra119, 2012.
32. Smith, D.H., Soares, H.D., Pierce, J.S., *et al.* A model of parasagittal controlled cortical impact in the mouse: cognitive and histopathologic effects. J Neurotrauma **12,** 169, 1995.
33. Yardeni, T., Eckhaus, M., Morris, H.D., Huizing, M., and Hoogstraten-Miller, S. Retro-orbital injections in mice. Lab Anim **40,** 155, 2011.
34. Mostany, R., and Portera-Cailliau, C. A craniotomy surgery procedure for chronic brain imaging. J Vis Exp 680, 2008. DOI: 10.3791/680.
35. Holtmaat, A., Bonhoeffer, T., Chow, D.K., *et al.* Long-term, high-resolution imaging in the mouse neocortex through a chronic cranial window. Nat Protoc **4,** 1128, 2009.
36. Stewart, P.A., Farrell, C.R., Farrell, C.L., and Hayakawa, E. Horseradish peroxidase retention and washout in blood-brain barrier lesions. J Neurosci Methods **41,** 75, 1992.
37. Chen, S. Time course of cellular pathology after controlled cortical impact injury. Exp Neurol **182,** 87, 2003.
38. Villapol, S., Loane, D.J., and Burns, M.P. Sexual dimorphism in the inflammatory response to traumatic brain injury. Glia **65,** 1423, 2017.
39. Kochanek, P.M., Marion, D.W., Zhang, W., *et al.* Severe controlled cortical impact in rats: assessment of cerebral edema, blood flow, and contusion volume. J Neurotrauma **12,** 1015, 1995.
40. Onyszchuk, G., Al-Hafez, B., He, Y.-Y., *et al.* A mouse model of sensorimotor controlled cortical impact: characterization using longitudinal magnetic resonance imaging, behavioral assessments and histology. J Neurosci Methods **160,** 187, 2007.
41. Onyszchuk, G., He, Y.-Y., Berman, N.E.J., and Brooks, W.M. Detrimental effects of aging on outcome from traumatic brain injury: a behavioral, magnetic resonance imaging, and histological study in mice. J Neurotrauma **25,** 153, 2008.
42. Glushakova, O.Y., Johnson, D., and Hayes, R.L. Delayed increases in microvascular pathology after experimental traumatic brain injury are associated with prolonged inflammation, blood–brain barrier disruption, and progressive white matter damage. J Neurotrauma **31,** 1180, 2014.
43. O'Connor, C.A., Cernak, I., and Vink, R. Both estrogen and progesterone attenuate edema formation following diffuse traumatic brain injury in rats. Brain Res **1062,** 171, 2005.
44. Huang, Z.G., Xue, D., Preston, E., Karbalai, H., and Buchan, A.M. Biphasic opening of the blood-brain barrier following transient focal ischemia: effects of hypothermia. Can J Neurol Sci J Can Sci Neurol **26,** 298, 1999.
45. Chodobski, A., Zink, B.J., and Szmydynger-Chodobska, J. Blood–brain barrier pathophysiology in traumatic brain injury. Transl Stroke Res **2,** 492, 2011.
46. Karve, I.P., Taylor, J.M., and Crack, P.J. The contribution of astrocytes and microglia to traumatic brain injury: neuroinflammation and TBI. Br J Pharmacol **173,** 692, 2016.
47. Öztas, B., and Kaya, M. Influence of orchidectomy and ovariectomy on the blood-brain barrier permeability during bicuculline-induced seizures. Horm Metab Res **30,** 500, 1998.
48. Öztaş, B., Küçük, M., and Kaya, M. Sex-dependent changes in blood–brain barrier permeability in epileptic rats following acute hyperosmotic exposure. Pharmacol Res **43,** 469, 2001.
49. Sohrabji, F. Guarding the blood–brain barrier: a role for estrogen in the etiology of neurodegenerative disease. Gene Expr **13,** 311, 2006.
50. Roof, R.L., and Hall, E.D. Gender differences in acute CNS trauma and stroke: neuroprotective effects of estrogen and progesterone. J Neurotrauma **17,** 367, 2000.
51. Bramlett, H.M., and Dietrich, W.D. Neuropathological protection after traumatic brain injury in intact female rats versus males or ovariectomized females. J Neurotrauma **18,** 891, 2001.
52. Stein, D.G. Brain damage, sex hormones and recovery: a new role for progesterone and estrogen? Trends Neurosci **24,** 386, 2001.
53. Grossman, K.J., and Stein, D.G. Does endogenous progesterone promote recovery of chronic sensorimotor deficits following contusion to the forelimb representation of the sensorimotor cortex? Behav Brain Res **116,** 141, 2000.
54. Rubenstein, R., Chang, B., Grinkina, N., *et al.* Tau phosphorylation induced by severe closed head traumatic brain injury is linked to the cellular prion protein. Acta Neuropathol Commun **5,** 30, 2017.
55. Farin, A., Deutsch, R., Biegon, A., and Marshall, L.F. Sex-related differences in patients with severe head injury: greater susceptibility to brain swelling in female patients 50 years of age and younger. J Neurosurg **98,** 32, 2003.

56. Covassin, T., Elbin, R.J., Harris, W., Parker, T., and Kontos, A. The role of age and sex in symptoms, neurocognitive performance, and postural stability in athletes after concussion. Am J Sports Med **40,** 1303, 2012.
57. Wagner, A.K., Willard, L.A., Kline, A.E., *et al.* Evaluation of estrous cycle stage and gender on behavioral outcome after experimental traumatic brain injury. Brain Res **998,** 113, 2004.
58. Maghool, F., Khaksari, M., and Khachki, A.S. Differences in brain edema and intracranial pressure following traumatic brain injury across the estrous cycle: involvement of female sex steroid hormones. Brain Res **1497,** 61, 2013.
59. Fortress, A.M., Avcu, P., Wagner, A.K., Dixon, C.E., and Pang, K.C.H. Experimental traumatic brain injury results in estrous cycle disruption, neurobehavioral deficits, and impaired GSK3β/β-catenin signaling in female rats. Exp Neurol **315,** 42, 2019.
60. Hohl, A., Zanela, F.A., Ghisi, G., *et al.* Luteinizing hormone and testosterone levels during acute phase of severe traumatic brain injury: prognostic implications for adult male patients. Front Endocrinol **9,** 29, 2018.

Address correspondence to:
Sarah E. Stabenfeldt, PhD
School of Biological and Health Systems Engineering
Ira A. Fulton Schools of Engineering
Arizona State University
Tempe, AZ 85287
USA

E-mail: sarah.stabenfeldt@asu.edu

Received: February 6, 2020
Accepted: April 9, 2020
Online Publication Date: July 15, 2020